


Article

The Influence of Dew Retting on the Mechanical Properties of Single Flax Fibers Measured Using Micromechanical and Nanomechanical Approaches

Ali Reda ¹, Thomas Dargent ¹, Louis Thomas ¹, Sebastien Grec ², Lionel Buchaillot ¹ and Steve Arscott ^{1,*}

¹ UMR 8520—IEMN—Institut d'Electronique de Microélectronique et de Nanotechnologie, University Polytechnique Hauts-de-France, Centrale Lille, CNRS, University Lille, 59000 Lille, France; ali.reda@univ-lille.fr (A.R.); thomas.dargent@univ-lille.fr (T.D.); louis.thomas@iemn.fr (L.T.); lionel.buchaillot@univ-lille.fr (L.B.)

² UMR 8576—UGSF—Unité de Glycobiologie Structurale et Fonctionnelle, CNRS, University Lille, 59000 Lille, France; sebastien.grec@univ-lille.fr

* Correspondence: steve.arscott@univ-lille.fr

Abstract: The mechanical properties of single flax fibers are characterized here as a function of dew retting. The fibers are measured using micromechanical and nanomechanical techniques over a large retting period (91 days). Damage-free single flax fibers in various stages of dew retting were manually extracted from retted flax plant stems. The flexural modulus and strength of the flax fibers were determined using micromechanical methods. The effective modulus of the outer surface of the single fibers was measured using AFM-based nanoindentation. The micromechanical methods revealed that the flexural modulus and strength of the manually extracted single fibers does not vary significantly as the retting progresses. The micromechanical methods revealed two distinct values of flexural strength in the fibers attributed to different failure modes. The values of these strengths do not vary significantly with retting or over-retting. The nanomechanical methods revealed that the effective modulus of the outer surface of the single fibers does evolve with retting. The physical/chemical origin of these observations remains to be established and could be the objective of future work.

Keywords: flax fibers; dew retting; mechanical properties; static and dynamic micromechanics; AFM-based nanoindentation; atomic force microscopy (AFM)



Citation: Reda, A.; Dargent, T.; Thomas, L.; Grec, S.; Buchaillot, L.; Arscott, S. The Influence of Dew Retting on the Mechanical Properties of Single Flax Fibers Measured Using Micromechanical and Nanomechanical Approaches. *Fibers* **2024**, *12*, 91. <https://doi.org/10.3390/fib12100091>

Academic Editor: Vincenzo Fiore

Received: 26 August 2024

Revised: 14 October 2024

Accepted: 16 October 2024

Published: 18 October 2024



Copyright: © 2024 by the authors. Licensee MDPI, Basel, Switzerland. This article is an open access article distributed under the terms and conditions of the Creative Commons Attribution (CC BY) license (<https://creativecommons.org/licenses/by/4.0/>).

1. Introduction

Flax fibers are considered a good natural material for use in many products ranging from textiles to composite materials [1]. Flax fibers grow on the outer tissue of the flax plant stem and must be separated from the stem materials for use. This mechanical separation of the fibers from the stem is facilitated by a traditional process known as retting [2,3]. Dew retting is a natural biological process that involves uprooting the stems and leaving them in the field for a period of time. The retting leads to a breaking down of the inter-fiber materials (middle lamella). It involves selective degradation of the plant cell wall polymers by microorganisms [4,5]. It has previously been determined that the composition of parietal polymers changes dramatically during retting, with a drastic decrease in the polymers of the middle lamella and primary cell wall (pectin/hemicellulose) [1]. A relative increase in crystalline cellulose in the fibers has also been observed, through a decrease in the amorphous form during the retting, which seems to translate into an increase in their mechanical strength [1,2]. It appears to be clear that the degree of retting plays a key role in the overall yield and quality of the resulting product [3,6]; both under-retting and over-retting resulting in poor fiber yield and poor fiber quality. Moreover, the fiber homogeneity depends very much on retting [7]. Under-retting means that fiber extraction is difficult as the inter-fiber tissue is not degraded enough to facilitate mechanical extraction

using machinery. Over-retting can result in low fiber quality thought to be due to excessive biological processes and weathering acting on the fibers. It has long been known that, depending on environmental conditions during the retting period, there is an optimum retting point where the extracted fiber quality is good and fiber extraction is easy. High fiber quality, e.g., good mechanical properties, is important to make high quality products.

To date, two main approaches have been used to study the mechanical properties of flax fibers: first, tensile testing to measure the bulk properties (elastic modulus and strength) [8–12], and second, nanoindentation of the cross-section of flax stems containing the fiber bundles to gain local internal mechanical information of the fiber [3–5]. In terms of tensile testing, the approach can result in large dispersion of results meaning data trends may not be visible. The origin of the relatively large dispersion of results is likely due to two factors: (i) industrial extraction of fibers can lead to fiber damage and (ii) tensile testing requires relatively long fibers (>1 cm), increasing the probability of damage being present. In terms of nanoindentation of the fiber cross-section, sample preparation is cumbersome and requires the use of a hard-embedded resin. The resin embedding approach is also time-consuming and not compatible with a real-time study of retting—as is the objective here. These problems have been pointed out by several authors [6–8].

In this study, to avoid some of the problems above, we use original micromechanical and nanomechanical methods developed by the authors to characterize the mechanical properties of manually extracted, pristine (uniform and defect-free) single flax fibers in different stages of dew retting. Measurements are performed on fibers over a whole retting cycle lasting 91 days in summer 2022. Our findings suggest that the physicochemical changes already described in the literature [1] might be reflected by the cell wall mechanical surface properties of the fiber with a reduced measurement dispersion.

2. Materials and Methods

2.1. Materials

Retted flax stems (Family: Linaceae; Genus: *Linum*; Species: *L. usitatissimum*; Variety: Felice) were collected from a field located in Killém, Northern France, run by the Van Robaey Frères company (VRF). The retting period studied lasted 91 days during summer/autumn 2022. The optimum retting time—when the flax stems are ready to be transferred to the factory for mechanical extraction of the fibers—was defined by VRF using artisanal means to be 56 days after harvesting. Retted flax stems were collected at different retting periods: (i) The under-retting period is defined from harvesting until the optimum retting point. (ii) The optimum retting point is estimated by VRF to be 56 days after the harvesting. (iii) The over-retting period lasts 4 weeks after the optimum retting point and ends 91 days after the day of harvesting.

2.2. Methods

2.2.1. Single-Flax-Fiber Manual Extraction Method

In the laboratory, flax fibers samples were manually extracted from the center of the flax stems. The single-fiber extraction process requires a lot of care in order to keep the fiber as straight as possible to avoid inducing any mechanical stress which could cause damage. The details of the method can be found in Refs. [13,14]. Briefly, to achieve this, a slight break was first made at the top of the flax stem. This slight break was able to expose the external tissue which was then carefully peeled out from the internal structure of the stem. Subsequently, a fiber bundle was peeled out from the external tissue by the aid of a pair of precision tweezers. A digital optical microscope (Keyence, Osaka, Japan) was used to help identify pristine single flax fibers within the bundle. Once a straight single flax fiber was identified, it was carefully held on one end using tweezers and the rest of the bundle was peeled off. This technique enabled long (~cm), straight, undamaged flax fibers to be isolated for experimentation. Note that the pristine condition of such single fibers is likely to be different to that of fibers which have been extracted using industrial means.

2.2.2. Polypropylene/Flax Fiber-Based Cantilever Sample Preparation

To create flax fiber-based cantilever samples for experimentation, the extracted single flax fibers were attached to the edge of polypropylene supports (measuring $6\text{ mm} \times 6\text{ mm} \times 100\text{ }\mu\text{m}$) using an adhesive tape (measuring $2\text{ mm} \times 2\text{ mm}$). The details of the cantilever fabrication can be found in Refs. [13,14]. For accurate measurements, certain key factors must be taken into consideration: uniformity of the single flax fibers, accurate alignment of the adhesive tape, and the perpendicular protrusion of the single-flax-fiber-based cantilever from the polypropylene chip. To assess these factors, the extracted fibers were examined using the digital optical microscope. Figure 1 shows an example of the flax fiber-based cantilevers on polypropylene support chips.

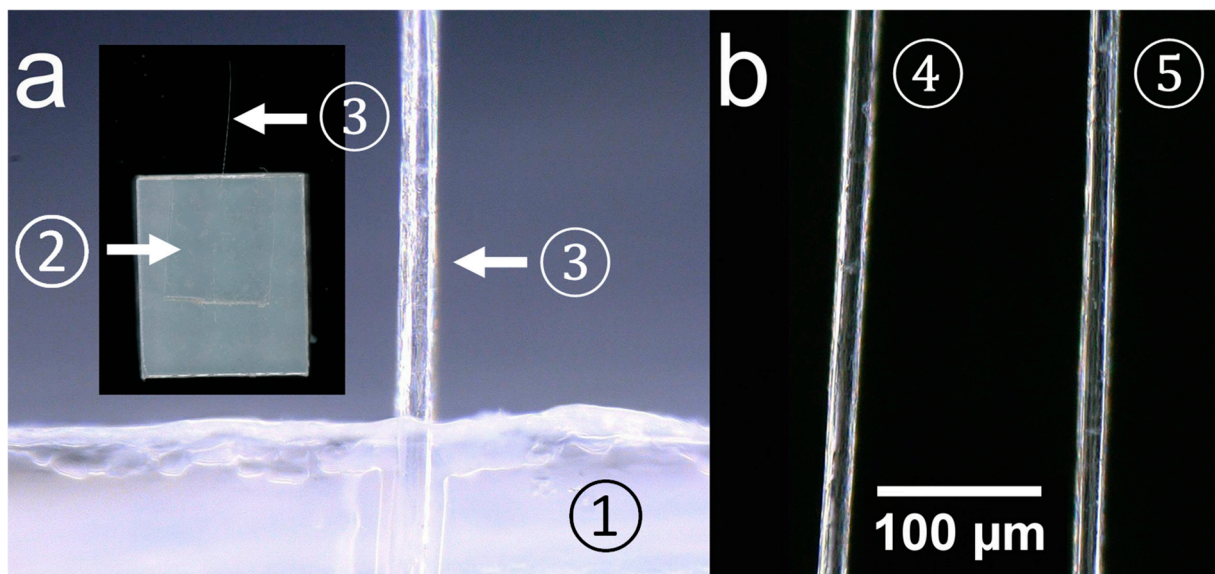


Figure 1. Single-flax-fiber microcantilever sample. (a) An example of the edge-to-edge alignment of the flax fiber cantilever/polypropylene sample. ① Polypropylene chip, ② adhesive tape, and ③ single flax fiber (uniform and defect-free). The inset shows a top view of the fiber cantilever/polypropylene chip. (b) Top view of the single-flax-fiber-based cantilever ④. Lateral view of the single-flax-fiber-based cantilever ⑤. The inset to the left illustrates the uniformity of fiber diameter along the fiber.

Figure 1a shows an optical microscopic image of the edge alignment of the anchoring adhesive tape to the edge of the polypropylene support. Figure 1b shows a top and lateral views of the flax fiber-based cantilever. These figures are used to measure the diameter to assess the fiber uniformity. Fiber uniformity is assessed if the diameter remains constant along the fiber length. Thirty diameter measurements are taken along the whole fiber length to determine the average fiber diameter. In this example, the average fiber diameter is $17.7 \pm 2.2\text{ }\mu\text{m}$. Note that only uniform-thickness fibers were selected for this study; this is a major advantage of our micromechanical approach over macroscopic tensile testing which uses long fibers. Moreover, Figure 1 shows that single, defect-free fibers were used in this study.

2.2.3. Dynamic Micromechanical Measurement of the Flexural Modulus of Single Flax Fibers

The main objective of this method was to accurately evaluate the flexural modulus of the manually extracted undamaged single flax fibers as a function of retting. In this way, the modulus reflects the modulus of the fiber in the stem rather than after being industrially extracted. The flexural modulus of the flax fibers was measured using a technique developed by the authors; details of the method can be found in Ref. [13]. Briefly, a high-speed camera (HSC) is used to capture the vibrations of the flax fiber-based cantilever.

The resulting images are then analyzed using software [15] to give the transient response of the vibrating flax fiber. By fitting an exponentially decaying sinusoidal damping function to the experimental transient response data, the resonant frequency can be extracted. Modeling can then determine the flexural modulus of the fiber.

The flax fiber-based cantilever/polypropylene samples were placed in a setup consisting of a high-speed camera (HSC) in an air environment (Vision Research, Wayne, IL, USA, 1280 by 800 pixels, frame rate = 3260). The method is illustrated in Figure 2.

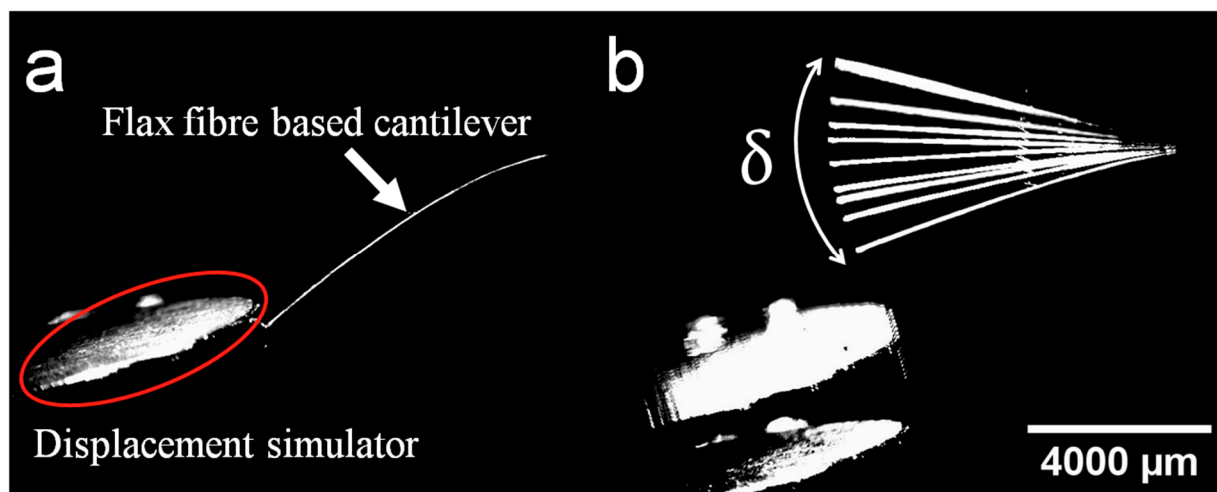


Figure 2. Determining the flexural modulus of a flax fiber using a vibrating microcantilever technique. (a) The fiber is deflected and (b) its transient response is recorded using a high-speed camera.

Firstly, flax fiber-based cantilevers were carefully displaced from the equilibrium position using a displacement tool marked by the red circle in Figure 2a. When the displacement tool is released, the fiber-based cantilever vibrates with decreasing amplitude as shown in Figure 2b. These vibrations are captured by the HSC. Subsequently, the resulting photos are analyzed using software [15] to extract the deflections of the fibers. In this way, a plot of the transient response of the single fiber can be made and subsequently fitted using a mechanical model to extract the mechanical modulus.

2.2.4. Static Micromechanical Measurements of the Flexural Strength of Single Flax Fibers

The main objective of this method was to evaluate the flexural strength of the flax fibers as a function of the retting period. In this way, the measured mechanical strength reflects the strength of the fiber in the stem rather than after being industrially extracted. The flexural strength of the flax fibers was measured using a technique developed by the authors [14]. Briefly, the flax fiber-based microcantilever is deflected until it fails. The failure is recorded using digital optical microscopy. The resulting image of the fiber just before failure is analyzed using software [15] to compute its maximum curvature. The maximum curvature is used in the analytical modeling to enable an extraction of the flexural strength of the fiber. For this part of the work, the flax fiber-based microcantilevers were fabricated in the same way as explained above in Section 2.2.2.

2.2.5. Atomic Force Microscopy (AFM) and AFM-Based Nanoindentation Measurements on the Surface of Single Flax Fibers

First, atomic force microscopy (AFM) measurements were carried out on the lateral surface of the single flax fibers to assess how their morphology varies with retting. Second, AFM-based nanoindentation measurements were also performed on the lateral surface of the single flax fibers to assess how the mechanical properties of the outer surface of the fibers evolve with retting. Note that our approach here differs from others in that we analyze the surface properties of single flax fibers in their natural state and as a function of

retting. By this we mean (i) manually extracted, pristine single fibers rather than industrially obtained fibers and (ii) fibers which are free from resin or extraneous compounds. Another originality of the approach here is that we measure the lateral surface of the flax fiber rather than a cut end. In this way, we probe the surface of the flax fiber which is most exposed to the retting of the middle lamella.

Retted single flax fibers were attached horizontally to silicon wafers using adhesive tape. This configuration exposes the lateral surface of the single flax fiber to the AFM probe. Then, 1 cm by 1 cm silicon chips are cut from silicon wafers (400 μm thick). These chips are then cleaned with isopropanol in a controlled environment (a class ISO6 cleanroom). Following the chip preparation, the individual flax fibers are placed on the silicon chips. The ends of these flax fibers are fixed to the chips with adhesive tape. After this assembly, the single flax fiber/chip sample is examined under a digital microscope. The optical microscope aided in verifying the precise alignment of the fiber on the chip. It is essential that the fiber lays straight and in contact with the silicon surface for the measurements. Figure 3 shows an illustration of the method used to fabricate a single flax fiber/chip sample.

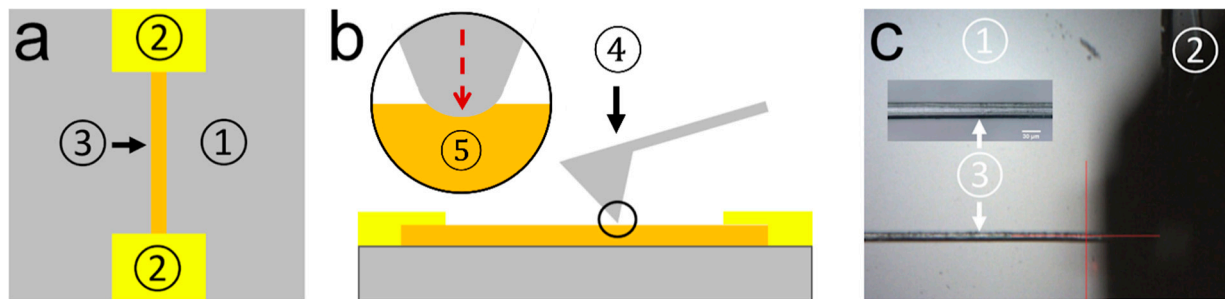


Figure 3. AFM and AFM-based nanoindentation of flax fibers in a lateral setup. (a) Top view of fiber (orange) attached to a silicon chip (gray) using adhesive tape (yellow). (b) Side view of the chip with the flax fiber being probed by the AFM tip. The inset in the black circle shows the AFM tip indenting the top surface of the single flax fiber sample. (c) Optical microscopy image of a flax fiber mounted on a silicon chip for AFM-based nanoindentation testing. The red cross shows the indentation point. The numbers in the figure show the ① silicon substrate, ② adhesive tape, ③ single flax fiber, ④ AFM tip, and ⑤ flax fiber surface.

Before indenting the single flax fiber horizontal surface, inverse optical sensitivity of the cantilever was measured on a PFQNM-SMPKIT-12M sapphire sample (Bruker, Billerica, MA, USA). A TAP525A probe with a tip radius of 120 nm performed blind tip estimation from images of a PA01 calibration sample (MikroMasch, Sofia, Bulgaria). The probe had a spring constant of 107 N/m. The maximum indenting depth of all measurements was 40 nm. Data were fitted by a Hertzian model with MountainsMap version 9.2 software (Digitalsurf, Besançon, France). During the fitting process, the coefficient of determination of the fit, denoted as R^2 , was carefully recorded while extracting the effective modulus E^* from the fitted data.

From the experimental data, 676 measurements were able to be fitted with the model having $R^2 > 0.98$. The data indicated that the effective mechanical moduli appeared to have distinct values. Therefore, the data were potted in histogram format to reveal this. To achieve this, binning of the modulus data is required. The choice of bin is important. If the bin is too large, details are missed; if the bin is too small, the data become noisy and difficult to understand. We therefore modified and optimized the bin size to make the details of the data apparent.

3. Results and Discussion

3.1. Dynamic Micromechanical Measurements of the Flexural Modulus of Single Flax Fibers as a Function of Dew Retting Period

Figure 4 shows examples of the transient response of single-flax-fiber-based micro-cantilevers for three stages of retting: an under-retted fiber, i.e., <35 days (Figure 4a), an optimally retted fiber, i.e., 56 days (Figure 4b), and an over-retted fiber, i.e., 63 to 91 days (Figure 4c). In Figure 4, the left panels show the complete transient response and the right panels show the transient response only in the low-deflection regime of the microcantilever [13]. The open red circles present the raw data extracted from the fiber vibration (see methods above). The damped harmonic system model is fitted to the raw data; this is shown by the red line in Figure 4.

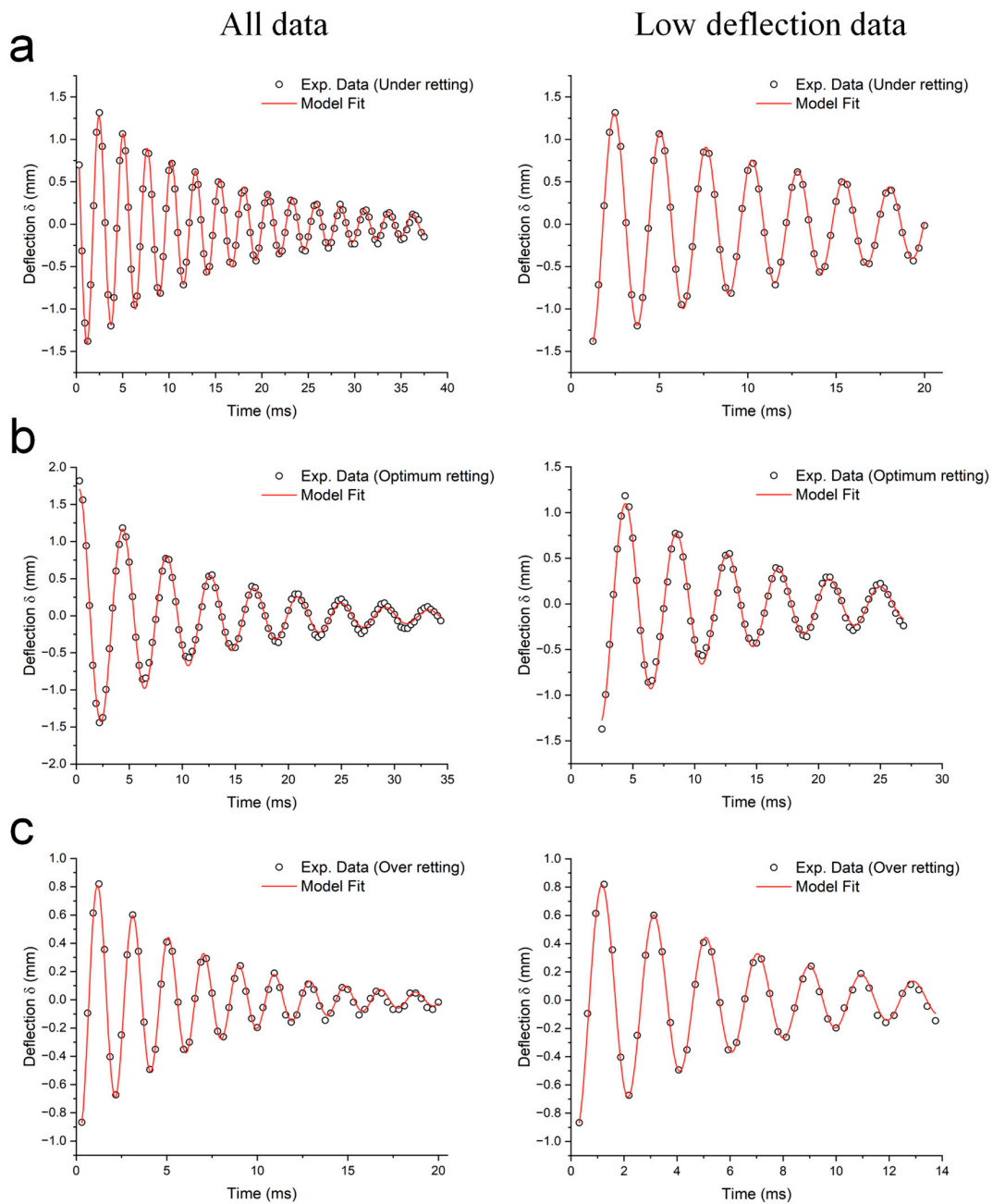


Figure 4. Examples of the transient response of single-flax-fiber-based cantilevers obtained using micromechanical tests. Result for flax fibers which were extracted from (a) under-retting, (b) optimal retting, and (c) over-retting periods.

First, the plots in Figure 4 show that the transient responses of the vibrating fibers can be accurately modeled by a simple damping harmonic system [13]. Second, the plots in Figure 4 can be used to extract the natural harmonic frequency associated with the vibration in the low-deflection regime; this is a crucial factor in determining the flexural modulus of the fiber as a whole, i.e., a heterogeneous structure. As explained in the methods above, by determining the harmonic frequency and having accurate knowledge of the cantilever dimensions, one can compute the modulus of the heterogeneous fiber as a whole [13].

Figure 5 shows a plot of the average flexural modulus of flax fibers as function of the retting period.

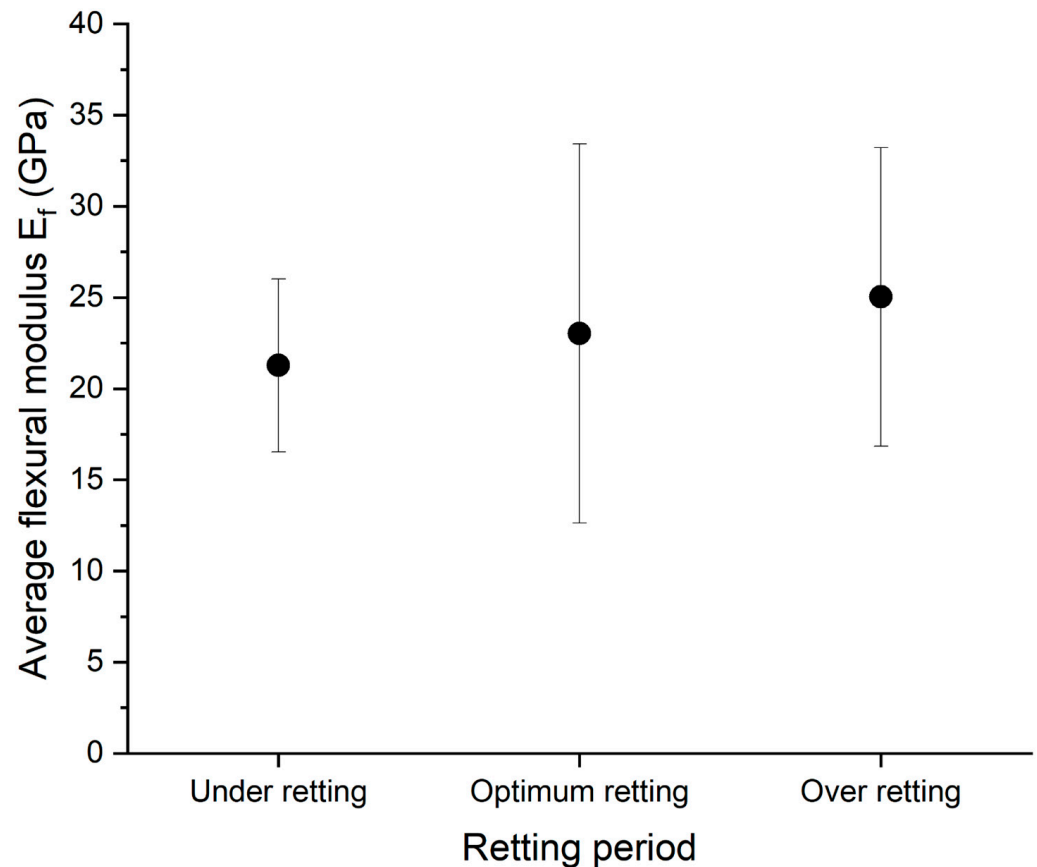


Figure 5. Plot of the evolution of the average flexural modulus of single, damage-free, manually extracted flax fibers as a function of retting. The data were obtained using micromechanical measurements.

The average flexural moduli extracted from the various retting stages were determined to be 22.2 ± 4.9 GPa (under-retting), 24.0 ± 10.8 GPa (optimum retting), and 26.1 ± 8.5 GPa (over-retting). The results suggest that the average flexural modulus of these manually-extracted, single, damage-free flax fibers remains relatively constant over the retting period.

3.2. Static Micromechanical Measurements of the Flexural Strength of Single Flax Fibers as a Function of Dew Retting Period

Figure 6 shows the plot of the average flexural strength of single flax fibers in the over-retting period. As explained in the methods, these measurements are obtained using static micromechanical means, the details of which can be found in [14].

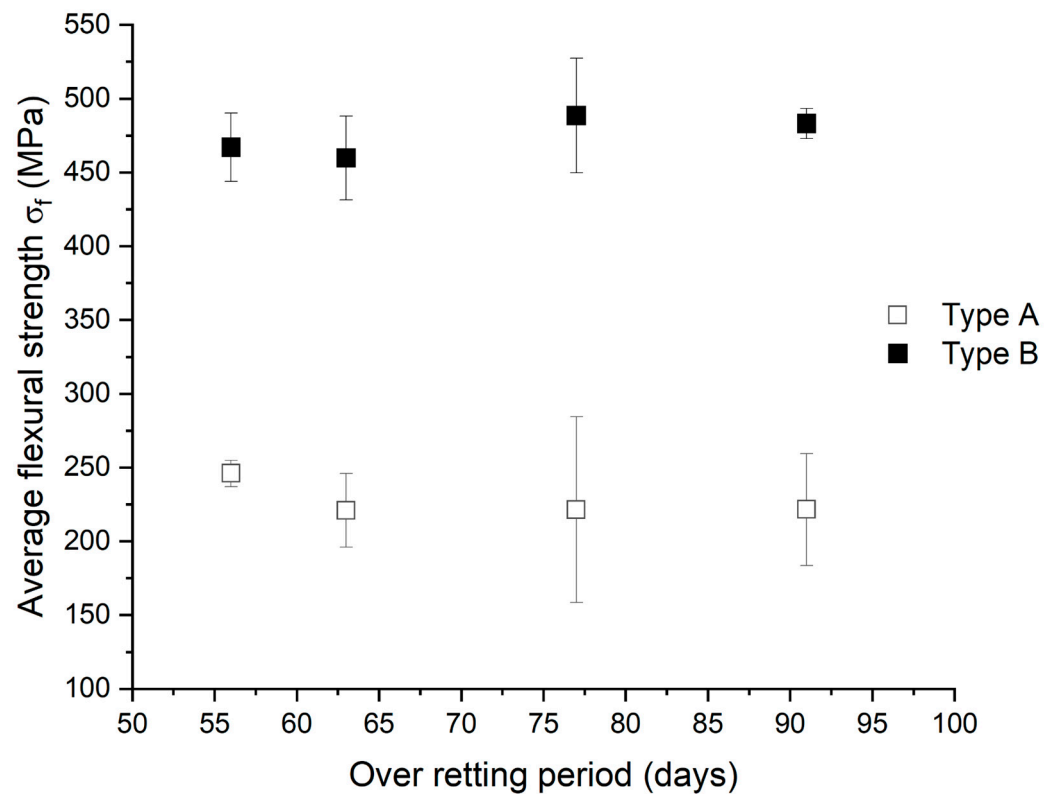


Figure 6. Plot of the evolution of the average flexural strength of flax fibers as a function of over-retting. Type A refers to failure via mechanically induced visible kink bands; Type B refers to failure with no visible kink-band formation. The data were obtained using micromechanical measurements.

The micromechanical measurements enable the observation of two types of failure. These two types (A and B) correspond to failure with and without kink-band formation [14]. Figure 6 suggests that the average flexural strengths are observed to be relatively constant as a function of over-retting (56–91 days). The average flexural strength measured at the optimum retting point (56 days after harvesting) is 245.9 ± 8.9 MPa (Type A) and 467.0 ± 23.1 MPa (Type B). With the advancement of retting, the flexural strength measured after 63 days from harvesting is 220.9 ± 25.0 MPa (Type A) and 459.8 ± 28.4 (Type B). After another week of retting (equal to 77 days from harvesting), the flexural strength was measured to be 221.4 ± 62.9 MPa (Type A) and 488.5 ± 38.9 MPa (Type B). At the final retting stage in this study (equal to 91 days after harvesting), the flexural strength measured 221.5 ± 38.0 MPa (Type A) and 483.1 ± 10.2 MPa (Type B). Moreover, the average flexural strength resulted from individual points along the retting period of Type A and Type B, similar to the flexural strength values obtained from fibers taken from the same stems as well as the same bunch of stems reported in our recent study [14]. This indicates that the static deflection method we developed can accurately determine the flexural strength of flax fibers with relatively low dispersion of results.

It is interesting to compare our results with those of others. Using traditional tensile testing of long fibers, studies have found that the tensile mechanical properties of extracted flax fibers can vary as a function of the degree of retting [5,16]. Martin et al. [17] showed that increasing retting (over 19 days) leads to an increase in the tensile modulus of flax fibers from 38.6 ± 17.3 GPa to 55.6 ± 11.8 GPa and an increase in the tensile strength of flax fibers from 792 ± 374 MPa to 1036 ± 270 MPa. Ruan et al. [18] observed this trend using water-retted flax fibers in laboratory conditions. They measured the tensile modulus changing from 19.85 ± 2.59 GPa to 29.44 ± 3.20 GPa and the tensile strength changing from 377.76 ± 90.64 MPa to 567.26 ± 86.91 MPa over a 10-day period. In contrast, Dey et al. [19] observed the tensile strength of flax fibers to pass through a peak as water

retting progressed over 10 days. In their results, the tensile modulus rises and then becomes stable at ~28 GPa. Réquilé et al. [20] showed that dew retting had little effect on the tensile properties of hemp fibers. Lecoublet et al. [21] measured the tensile modulus of flax fibers as a function of retting. The authors point out the importance of differentiating between what they term as a 'continuous elementary fiber' and a 'long technical fiber', i.e., a sum of elementary fibers linked by pectins. For long technical fibers, they observed the tensile modulus to fall from 66.8 GPa to 41.3 GPa and the tensile strength to fall from 477 MPa to 224 MPa. For continuous elementary fibers, they observed the tensile modulus to increase from 68.9 GPa to 88.2 GPa, and the tensile strength to fall slightly from 631 MPa to 553 MPa. They concluded that the retting-induced degradation of the pectins in the technical fibers was responsible for the larger observed change in the tensile properties.

The weather conditions are also known to have an impact on the degree of retting of bast fibers [22]. The weather conditions during summer 2022 near the retting field can be found in the supplementary information. Summer 2022 involved a heatwave and a relatively dry over-retting period. These factors could have contributed to the conservation of the mechanical properties of the flax fibers beyond the optimum retting point.

Our findings suggest that retting is not significantly apparent in the micromechanical properties of the single flax fibers. However, it is well known that the main cause of retting is to break down (through enzyme activity) the middle lamella material between the fibers [23] and, in extreme cases of over-retting, the cell walls of the fibers [24–27]. Therefore, it seems reasonable to see whether it is possible to observe the influence of retting on the lateral surface of the flax fibers using near-field microscopy. Therefore, we decided to probe the lateral surface of the single fibers using AFM and AFM-based nanoindentation to observe the effect of retting on the fiber surface topography and mechanical properties.

3.3. AFM Measurements on the Lateral Surface of Flax Fibers as a Function of Retting Period

In this part of the study AFM was used to observe the topography of the lateral surface of single flax fibers as a function of retting. Our approach differs from others in that it reveals the free lateral surface of the fiber in its natural state, e.g., no resin is required. Our technique is also compatible with a real-time study as sample preparation is rapid.

Figure 7 shows examples of single fibers surface topography (upper images) and the corresponding phase (lower images) of the lateral surface of single flax fibers in three stages of retting: under-retted fibers, optimally-retted fibers, and over-retted fibers.

Figure 7a to the left, shows an example of the topography of the surface of a flax fiber extracted from the under-retting period. Figure 7a in the middle, shows a topography image of a flax fiber surface scan extracted from the optimal retting point and, Figure 7a, to the right shows a topographical example of a flax fiber surface extracted from the over-retting stage. The topographies in Figure 7a suggests that the fiber surface has a spaghetti-like structure. To gain better understanding of the flax fiber surface morphology, phase is recorded with the topographic images. Figure 7b shows the phase acquired simultaneously with the topographical image as a function of the retting period. Figure 7b to the left, shows that as a consequence of the morphology, the spaghetti-like structure is enhanced in phase images. As retting reaches the optimum point, no significant change exhibits in the fiber roughness as shown in Figure 7b in the middle. As retting advances in over-retting points the spaghetti like surface structure disappears as shown in Figure 7b to the right.

It is difficult to interpret the results, especially when compared to the trends that appear in the plots of Figures 5 and 6. However, both trends in Figure 7 show that the flax fiber surface is evolving with retting. Moreover, these topographical images can be used to extract the roughness of the flax fiber surface as a function of the retting period. Figure 8 shows a plot of the roughness as a function of retting period.

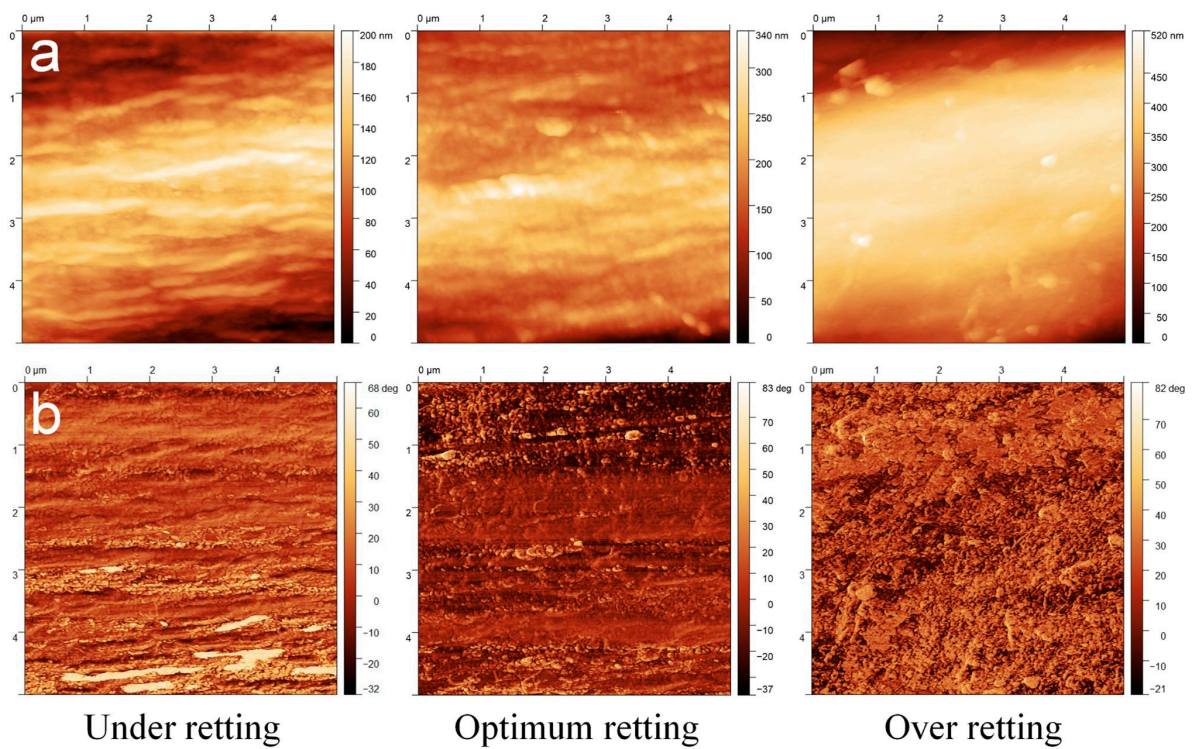


Figure 7. AFM images of the lateral surface of single flax fibers in different stages of retting. (a) Topography images of the lateral surface of the flax fiber in under-retting (left), optimum retting (middle), and over-retting (right). To gain better understanding of the flax fiber surface morphology, phase is recorded with the topographic images. (b) Corresponding phase images of the topographical flax fiber lateral surface images as a function of the retting period. AFM images were processed with GWYDDION version 2.65 software.

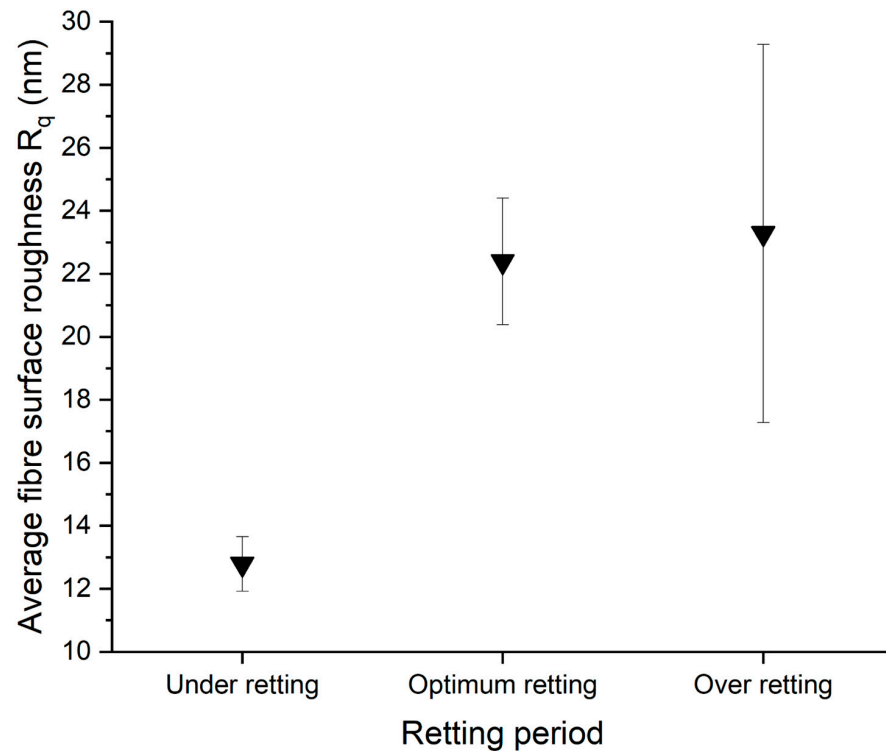


Figure 8. Measured roughness of the lateral surface of the single flax fibers plotted as a function of retting and post-retting time. The roughness (R_q) was obtained from the AFM topography measurements.

The plot in Figure 8 illustrates the evolution of the flax fiber roughness as a function of the retting period. The spatial cut-off frequency used to extract the roughness is $2.2 \mu\text{m}$. The average roughness of the flax fiber surface from a sample extracted from the under-retting point is $12.8 \pm 0.9 \text{ nm}$. As retting reaches the optimum point, the flax fiber roughness measures $22.4 \pm 2.0 \text{ nm}$. Furthermore, as retting advances to over-retting, the flax fiber roughness measures $23.3 \pm 6.0 \text{ nm}$. Therefore, the trend shown in the plot of Figure 8 suggests that the fiber roughness evolves as a function of retting. This suggests that there is an influence of retting on the flax fiber surface.

Note that gathering high-quality AFM images proved to be challenging. This was due to the presence of impurities on the fiber that are displaced as the tip scans. This means the resulting image has artifacts. Also, the macroscopic cylindrical shape of the fiber makes the overall imaging process more challenging than a flat surface. We could perform the measurements only on selected areas that looked clean on the optical microscope integrated within the AFM. Even in these selected areas, imaging was difficult (still some dust and large variations in height). Only images representative of the cleanest areas with the smoothest topography were considered.

3.4. AFM-Based Nanoindentation Measurements on Flax Fibers as a Function of Retting Period

In this part of the study, AFM-based nanoindentation was used to measure the mechanical properties of the lateral surface of single flax fibers as a function of retting. As we mentioned above, our approach reveals the free lateral surface of the fiber in its natural state.

Figure 9 shows histograms of the effective modulus of the surface of flax fibers as a function of retting obtained by analysis of the AFM-based nanoindentation data. The data in Figure 9 were obtained by fitting the raw AFM-based nanoindentation measurements to a Hertzian model [28]. Of the 676 modulus values, 650 measurements are used to plot Figure 9 to reveal the main peaks. Note that 26 measurements were excluded from the plot as they are outliers. The whole plots can be found in the Supplementary Information.

Figure 9 shows results from measurements on flax fibers in three different retting phases: under-retting (Figure 9a), optimal retting (Figure 9b), and over-retting (Figure 9c). Figure 9a shows histograms presenting the experimental data and the gaussian fits representing two distinct peaks resulting from the fitted data extracted from the under-retted phase. The red fit corresponds to peak 1 at $260.6 \pm 59.7 \text{ MPa}$, while the green fit corresponds to peak 2 at $466.3 \pm 46.7 \text{ MPa}$. As the retting process advances and the optimum retting point is reached, there is a noticeable shift in the data patterns as shown in Figure 9b. Peak 1 (red curve) undergoes a significant shift towards a lower value and is now recorded at $138.0 \pm 32.6 \text{ MPa}$. Peak 2 (green curve) experienced a reduction in the number of measurements compared to the under-retting stage and shifted towards $364.1 \pm 33.2 \text{ MPa}$. At the same time, a new peak, named peak 3 (yellow curve) appears at around $752.1 \pm 134.4 \text{ MPa}$. However, as retting progresses beyond the optimum phase, one single peak at a value of $201.1 \pm 24.9 \text{ MPa}$ is present, as shown in Figure 9c. These results strongly suggest that there is significant variation in the mechanical properties at the fiber surface as retting progresses. In order to better visualize these changes, Figure 10 shows a plot of the peaks resulting from the histogram data as a function of the retting period.

First, peak 1 (red diamonds) is common to the three retting phases that remains relatively constant, i.e., between 138 and 260 MPa. Second, peak 2 (green squares) present in the under-retted and the optimally retted fibers in the range of 364–466 MPa. This peak is not apparent in the over-retted samples. Finally, peak 3 (yellow circle) appeared at approximately 752 MPa, which is only visible in the optimally retted fibers. The over-retted fibers only have the peak centered at 201 MPa.

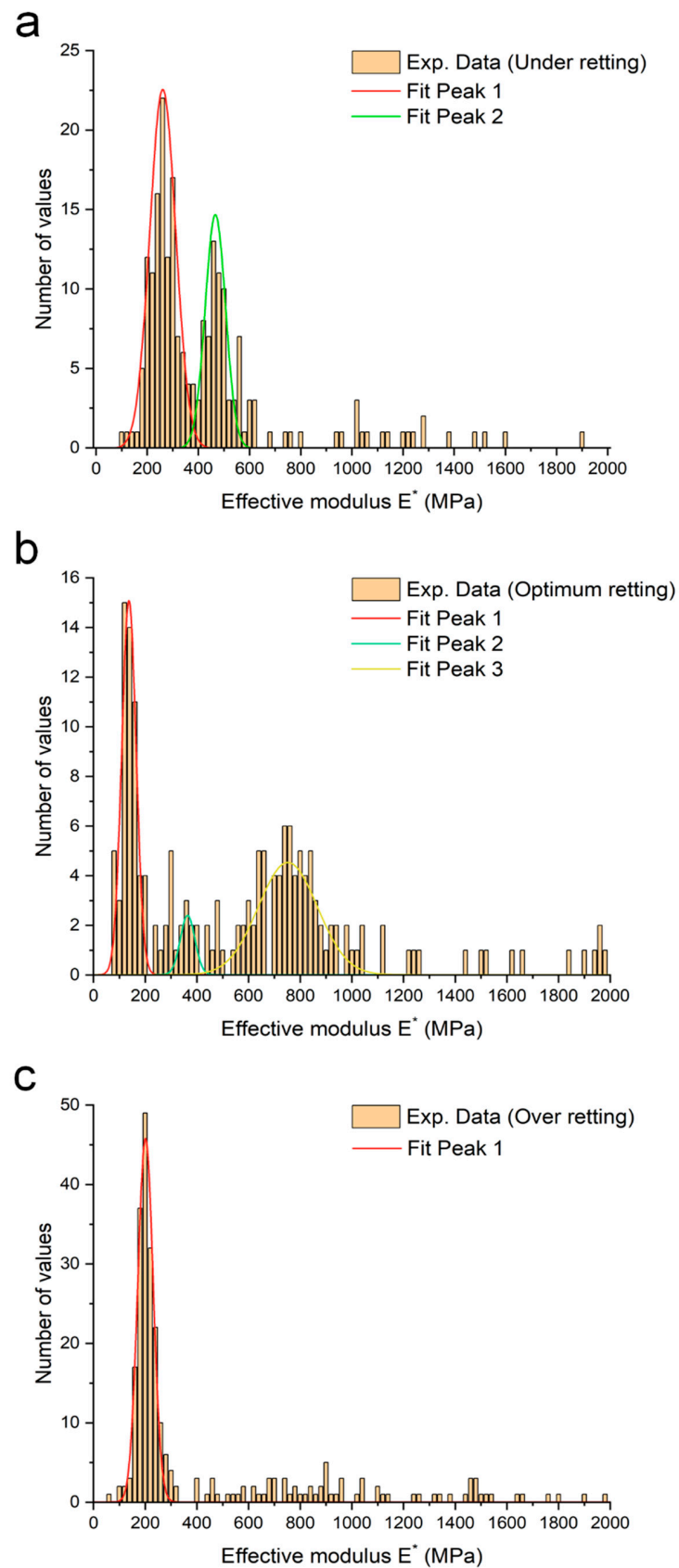


Figure 9. Histograms of the effective modulus of the surface of flax fibers as a function of retting: (a) under-retting, (b) optimal retting, and (c) over-retting. The results are obtained by AFM-based nanoindentation measurements.

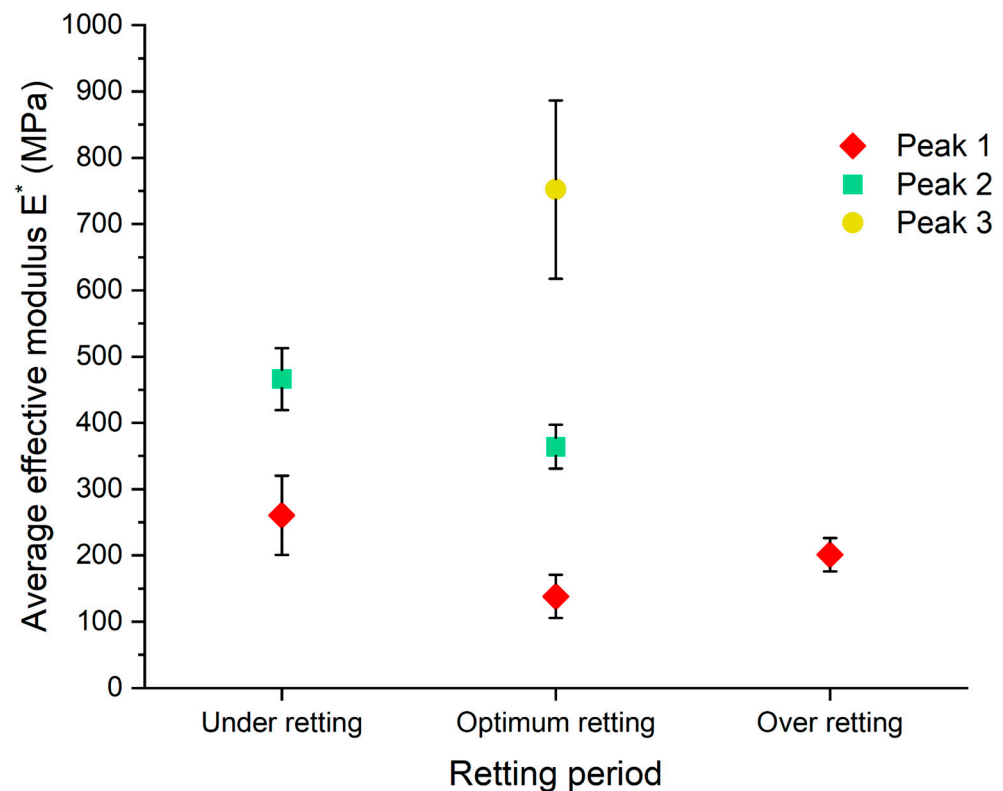


Figure 10. Plot of the average effective modulus (peaks) of the surface of single flax fibers as a function of the retting period. The results are obtained by AFM-based nanoindentation measurements. The error bars correspond to the FWHM of the peaks.

The data obtained using AFM-based nanoindentation measurements of the surface of the fibers evolve with progressive retting. However, this is not the case of the data obtained using the micromechanical means. In addition, there is an order of magnitude of difference between the values obtained via the two different means. This discrepancy is possibly due to the fact that the AFM-based nanoindentation value only represents the modulus at the fiber surface. Knowing that the thickness of the primary cell wall is $0.2 \mu\text{m}$ [9,29], in this AFM-based nanoindentation test, a depth of maximum value of 40 nm is indented. It is therefore clear that this measurement is specific to the surface of the primary cell wall and does not encompass the entirety of the fiber cell wall structure, and certainly not the fiber as a whole heterogeneous composite. The measurements here can be compared with work by others [30]. They used intermittent non-resonant contact measurements to semi-quantitatively measure the modulus of cross-sections of flax fibers embedded in resin. First, they clearly show that the resin is present in the lumen part of the fibers. Second, they report a modulus of around 20 GPa for the whole fiber, which agrees very well with our micromechanical measurements. Third, they report a much lower modulus in the tissue between the fibers, where the resin is unlikely to reach. This lower value $<1 \text{ GPa}$ seems to agree with our observations at the lateral wall of the fiber here.

Our results indicate that AFM-based nanoindentation has been able to indent the lateral surface of the flax fiber and produce a trend that clearly shows the influence of retting on the surface of the flax fiber as a function of the retting time. In addition, this technique significantly increases the surface area available for indentation, allowing the AFM probe to traverse and indent a larger area along the length of the flax fiber. As a result, this method effectively mitigates the limitations associated with resin-based methods and produces precise results.

Finally, given the lack of previous research and investigation in this specific area, particularly in relation to the indentation of the lateral surface of single fibers, we are faced

with the challenge of accurately identifying the exact material subjected to indentation. However, while a definitive identification remains elusive, we can propose possible hypotheses. One such hypothesis relates to the modulus of the polysaccharides found in the primary cell wall of the flax fiber. It is conceivable that the AFM-based nanoindentation measurements probe the mechanical properties of these polysaccharides. Alternatively, the measurements may include some polysaccharides that are either persistently attached to the fiber–middle lamella interface or are exposed after being degraded by enzymatic activity during the retting process. We can reasonably hypothesize that the action of the enzymes is not homogeneous, and that some pectin/hemicellulose polymers remain, modifying the mechanical properties of the surface. Further research and analysis is required to clarify this intriguing aspect of the study.

4. Conclusions

The mechanical properties of single flax fibers in various stages of dew retting can be determined using original micromechanical and nanomechanical means. The micromechanical means involve techniques using a single-flax-fiber-based microcantilever; the nanomechanical means use AFM-based nanoindentation to probe the outer lateral surface of the fibers. Single, uniform-diameter, defect-free flax fibers were obtained manually from flax stems rather than using industrial extraction methods. The micromechanical methods were successful in accurately determining the flexural modulus and flexural strength of single flax fibers as a function of retting period. The results suggest that there is no significant influence of the retting process on the flexural modulus or strength of manually extracted, damage-free single flax fibers over a wide retting period (from 1 to 91 retting days). The micromechanical methods were able to identify two different failure modes in bending flax fibers; one failure results in the formation of kink bands, and the other does not. The strength of these failure modes is different but does not evolve significantly with retting. The nanomechanical methods were successful in accurately determining the effective modulus of the lateral surface of single flax fibers as a function of retting period. Analysis of the data by fitting to a Hertzian model determined the statistical distribution of the effective surface modulus of the fibers. Different peaks at different values of moduli were apparent. These moduli peaks were observed to shift with increasing retting period. The values of the moduli peaks were significantly less than the moduli obtained using the micromechanical means—something which measures the whole heterogeneous fibers rather than just the surface. We tentatively ascribe the variation in the fiber surface moduli (obtained using AFM-based nanoindentation) to the influence of retting on the inter-fiber material (middle lamella) and the fiber surface, e.g., a degradation of the primary cell wall with retting. Finally, our findings suggest that physicochemical changes to flax fibers, already reported in previous studies, are visible in the mechanical surface properties of the fiber.

Supplementary Materials: The following supporting information can be downloaded at <https://www.mdpi.com/article/10.3390/fib12100091/s1>, Figure S1: Histograms of the effective modulus of the surface of flax fibers as a function of retting: (a) under-retting, (b) optimal retting, and (c) over-retting. The results are obtained by AFM-based nanoindentation measurements. These plots are for all sorted experimental data. Figure S2: The weather data for Killem, France, during the period of 6th July to 1st October. The retting period (as defined by VRF) was from 6th July to 31st August. The optimum retting day (29th of August) is defined by the orange color. The over-retting period was from the latter date to the 1st of October. (a) The data of air temperature, (b) rainfall (precipitation), (c) wind speed, and (d) direct sunlight (no cloud cover). Data available at <https://www.infoclimat.fr/climatologie-mensuelle/000R5/juillet/2022/bergues.html> (accessed on 15 October 2024).

Author Contributions: Conceptualization, A.R. and S.A.; methodology, A.R., T.D., L.T. and S.A.; validation, A.R., T.D., L.T. and S.A.; formal analysis, A.R., T.D., L.T. and S.A.; investigation, A.R., T.D., L.T. and S.A.; resources, T.D. and L.T.; data curation, A.R., T.D., L.T. and S.A.; writing—original draft preparation, A.R. and S.A.; writing—review and editing, A.R., T.D., L.T., S.G., L.B. and S.A.;

visualization, A.R. and S.A.; supervision, S.A., L.B. and S.G.; project administration, S.A., L.B. and S.G.; funding acquisition, L.B. and S.G. All authors have read and agreed to the published version of the manuscript.

Funding: CNRS funding of the 80 Prime ‘VAL project’ and for the PhD funding of AR. Part of the work was supported by IEMN/PCMP/PCP, part of RENATECH.

Data Availability Statement: Data underlying the results presented in this article may be obtained from the authors upon reasonable request.

Acknowledgments: The authors would like to thank the company Van Robaeys Frères (Killem, France) for allowing us to collect flax stem samples from their fields in the period of retting (summer/autumn 2022). The authors thank Jean-Michel Mallet (IEMN-CNRS, University of Lille) for the fabrication of the mechanical apparatuses used for the study. We thank Vincent Thomy (IEMN, University of Lille) for the loan of the high-speed camera.

Conflicts of Interest: The authors declare no conflicts of interest.

References

1. Yan, L.; Chouw, N.; Jayaraman, K. Flax Fibre and Its Composites—A Review. *Compos. Part B Eng.* **2014**, *56*, 296–317. [\[CrossRef\]](#)
2. Foulk, J.; Akin, D.; Dodd, R.; Ulven, C. Production of Flax Fibers for Biocomposites. In *Cellulose Fibers: Bio- and Nano-Polymer Composites*; Kalia, S., Kaith, B.S., Kaur, I., Eds.; Springer: Berlin/Heidelberg, Germany, 2011; pp. 61–95, ISBN 978-3-642-17369-1.
3. Baley, C.; Gomina, M.; Breard, J.; Bourmaud, A.; Drapier, S.; Ferreira, M.; Le Duigou, A.; Liotier, P.J.; Ouagne, P.; Soulat, D.; et al. Specific Features of Flax Fibres Used to Manufacture Composite Materials. *Int. J. Mater. Form.* **2019**, *12*, 1023–1052. [\[CrossRef\]](#)
4. Zhang, J.; Henriksson, H.; Szabo, I.J.; Henriksson, G.; Johansson, G. The Active Component in the Flax-Retting System of the Zygomycete *Rhizopus Oryzae* Is a Family 28 Polygalacturonase. *J. Ind. Microbiol. Biotechnol.* **2005**, *32*, 431–438. [\[CrossRef\]](#) [\[PubMed\]](#)
5. Akin, D.E. Linen Most Useful: Perspectives on Structure, Chemistry, and Enzymes for Retting Flax. *ISRN Biotechnol.* **2013**, *2013*, 186534. [\[CrossRef\]](#) [\[PubMed\]](#)
6. Réquillé, S.; Le Duigou, A.; Bourmaud, A.; Baley, C. Peeling Experiments for Hemp Retting Characterization Targeting Biocomposites. *Ind. Crop. Prod.* **2018**, *123*, 573–580. [\[CrossRef\]](#)
7. Tahir, P.M.; Ahmed, A.B.; SaifulAzry, S.O.A.; Ahmed, Z. Retting Process of Some Bast Plant Fibers and Its Effect on Fibre Quality: A Review. *BioResources* **2011**, *6*, 5260–5281. [\[CrossRef\]](#)
8. Baley, C. Analysis of the Flax Fibres Tensile Behaviour and Analysis of the Tensile Stiffness Increase. *Compos. Part Appl. Sci. Manuf.* **2002**, *33*, 939–948. [\[CrossRef\]](#)
9. Bos, H.L.; Van Den Oever, M.J.A.; Peters, O.C.J.J. Tensile and compressive properties of flax fibres for natural fibre reinforced composites. *J. Mater. Sci.* **2002**, *37*, 1683–1692. [\[CrossRef\]](#)
10. Andersons, J.; Sparrins, E.; Joffe, R.; Wallstrom, L. Strength Distribution of Elementary Flax Fibres. *Compos. Sci. Technol.* **2005**, *65*, 693–702. [\[CrossRef\]](#)
11. Gourier, C.; Le Duigou, A.; Bourmaud, A.; Baley, C. Mechanical Analysis of Elementary Flax Fibre Tensile Properties after Different Thermal Cycles. *Compos. Part Appl. Sci. Manuf.* **2014**, *64*, 159–166. [\[CrossRef\]](#)
12. Lefeuvre, A.; Bourmaud, A.; Morvan, C.; Baley, C. Elementary Flax Fibre Tensile Properties: Correlation between Stress–Strain Behaviour and Fibre Composition. *Ind. Crop. Prod.* **2014**, *52*, 762–769. [\[CrossRef\]](#)
13. Reda, A.; Dargent, T.; Arscott, S. Dynamic Micromechanical Measurement of the Flexural Modulus of Micrometre-Sized Diameter Single Natural Fibres Using a Vibrating Microcantilever Technique. *J. Micromech. Microeng.* **2024**, *34*, 015009. [\[CrossRef\]](#)
14. Reda, A.; Arscott, S. Static Micromechanical Measurements of the Flexural Modulus and Strength of Micrometre-Diameter Single Fibres Using Deflecting Microcantilever Techniques. *Sci. Rep.* **2024**, *14*, 2967. [\[CrossRef\]](#) [\[PubMed\]](#)
15. Schneider, C.A.; Rasband, W.S.; Eliceiri, K.W. NIH Image to ImageJ: 25 Years of Image Analysis. *Nat. Methods* **2012**, *9*, 671–675. [\[CrossRef\]](#)
16. Akin, D.E. Flax—Structure, Chemistry, Retting and Processing. In *Industrial Applications of Natural Fibres*; Müssig, J., Ed.; Wiley: Hoboken, NJ, USA, 2010; pp. 87–108, ISBN 978-0-470-69508-1.
17. Martin, N.; Mouret, N.; Davies, P.; Baley, C. Influence of the Degree of Retting of Flax Fibers on the Tensile Properties of Single Fibers and Short Fiber/Polypropylene Composites. *Ind. Crop. Prod.* **2013**, *49*, 755–767. [\[CrossRef\]](#)
18. Ruan, P.; Raghavan, V.; Garipey, Y.; Du, J. Characterization of Flax Water Retting of Different Durations in Laboratory Condition and Evaluation of Its Fiber Properties. *BioResources* **2015**, *10*, 3553–3563. [\[CrossRef\]](#)
19. Dey, P.; Mahapatra, B.S.; Pramanick, B.; Kumar, A.; Negi, M.S.; Paul, J.; Shukla, D.K.; Singh, S.P. Quality Optimization of Flax Fibre through Durational Management of Water Retting Technology under Sub-Tropical Climate. *Ind. Crop. Prod.* **2021**, *162*, 113277. [\[CrossRef\]](#)
20. Réquillé, S.; Goudenhooft, C.; Bourmaud, A.; Le Duigou, A.; Baley, C. Exploring the Link between Flexural Behaviour of Hemp and Flax Stems and Fibre Stiffness. *Ind. Crop. Prod.* **2018**, *113*, 179–186. [\[CrossRef\]](#)

21. Lecoublet, M.; Khennache, M.; Leblanc, N.; Ragoubi, M.; Poilâne, C. Physico-Mechanical Performances of Flax Fiber Biobased Composites: Retting and Process Effects. *Ind. Crop. Prod.* **2021**, *173*, 114110. [[CrossRef](#)]
22. Chabbert, B.; Philippe, F.; Thiébeau, P.; Alavoine, G.; Gaudard, F.; Pernes, M.; Day, A.; Kurek, B.; Recous, S. How the Interplay between Harvest Time and Climatic Conditions Drives the Dynamics of Hemp (*Cannabis sativa* L.) Field Retting. *Ind. Crop. Prod.* **2023**, *204*, 117294. [[CrossRef](#)]
23. Melelli, A.; Arnould, O.; Beaugrand, J.; Bourmaud, A. The Middle Lamella of Plant Fibers Used as Composite Reinforcement: Investigation by Atomic Force Microscopy. *Molecules* **2020**, *25*, 632. [[CrossRef](#)] [[PubMed](#)]
24. Pallesen, B.E. The Quality of Combine-Harvested Fibre Flax for Industrials Purposes Depends on the Degree of Retting. *Ind. Crop. Prod.* **1996**, *5*, 65–78. [[CrossRef](#)]
25. Akin, D.E.; Morrison, W.H.; Gamble, G.R.; Rigsby, L.L.; Henriksson, G.; Eriksson, K.-E.L. Effect of Retting Enzymes on the Structure and Composition of Flax Cell Walls. *Text. Res. J.* **1997**, *67*, 279–287. [[CrossRef](#)]
26. Akin, D.E.; Rigsby, L.L.; Henriksson, G.; Eriksson, K.-E.L. Structural Effects on Flax Stems of Three Potential Retting Fungi. *Text. Res. J.* **1998**, *68*, 515–519. [[CrossRef](#)]
27. Richely, E.; Bourmaud, A.; Placet, V.; Guessasma, S.; Beaugrand, J. A Critical Review of the Ultrastructure, Mechanics and Modelling of Flax Fibres and Their Defects. *Prog. Mater. Sci.* **2022**, *124*, 100851. [[CrossRef](#)]
28. Kontomaris, S.V.; Malamou, A. Hertz Model or Oliver & Pharr Analysis? Tutorial Regarding AFM Nanoindentation Experiments on Biological Samples. *Mater. Res. Express* **2020**, *7*, 033001. [[CrossRef](#)]
29. Goudenhoft, C.; Bourmaud, A.; Baley, C. Flax (*Linum usitatissimum* L.) Fibers for Composite Reinforcement: Exploring the Link Between Plant Growth, Cell Walls Development, and Fiber Properties. *Front. Plant Sci.* **2019**, *10*, 411. [[CrossRef](#)]
30. Arnould, O.; Siniscalco, D.; Bourmaud, A.; Le Duigou, A.; Baley, C. Better Insight into the Nano-Mechanical Properties of Flax Fibre Cell Walls. *Ind. Crop. Prod.* **2017**, *97*, 224–228. [[CrossRef](#)]

Disclaimer/Publisher’s Note: The statements, opinions and data contained in all publications are solely those of the individual author(s) and contributor(s) and not of MDPI and/or the editor(s). MDPI and/or the editor(s) disclaim responsibility for any injury to people or property resulting from any ideas, methods, instructions or products referred to in the content.